Apparatus for nonresonant rf power absorption studies in high T_c superconductors and CMR materials using rf oscillators

S. Sarangi[a)] and S. V. Bhat
Department of Physics, Indian Institute of Science, Bangalore-560012, India

The design, fabication, and performance of an apparatus for measurement of nonresonant rf power absorption (NRRA) in superconducting and CMR samples are described. The system consists of an effective self-resonant *LC* tank circuit driven by a NOT gate (Logic gate). The samples under investigation are placed in the core of an inductive coil and nonresonant power absorption is determined from the measured shift in total current supplies to the whole oscillator circuit. A customized low temperature insert is used to integrate the experiment with a commercial oxford cryostat and temperature controller. The system makes use of a sensitive digital multimeter (Keithley 2002 model) and is capable of measuring NRRA in superconducting and colossal magnetoresistance samples of volume as small as 1×10^{-3} cm^3 with a signal to noise ratio of 10. Further increase in the sensitivity of the experimental setup can be obtained by summing the results of repeated measurements obtained in the same temperature interval. The system has been tested for an IC 74LS04 oscillator at frequencies between 1 MHz and 25 MHz in the temperature range from 4.2 K to 400 K and in magnetic field from 0 to 1.4 T. The system performance is evaluated by measuring the NRRA in $YBa_2Cu_3O_7$ (YBCO) superconducting sample and $La_{0.7}Sr_{0.3}MnO_3$ (LSMO) colossal magnetoresistive (CMR) manganite samples at different rf frequencies. During a measurement all operation are controlled automatically by computer from a menu-driven software system, with user input required only on initiation of measurement sequence.

I. INTRODUCTION

Nonresonant radio frequency absorption (NRRA) and nonresonant microwave absorption (NRMA) are highly sensitive, noninvasive technique to detect and characterize the superconducting phase and identify grain boundary weak links. CW NMR and EPR spectrometers are generally used for NRRA and NRMA studies in rf and microwave respectively. It involves subjecting the sample to rf or microwave in a preferred orientation and scanning the magnetic field from negative to positive value through zero at fixed temperature below or above T_c.[1,2] It is observed that the magnetic field dependent losses in superconducting state of a sample give rise to an intense signal when studied using conventional continuous-wave (CW) nuclear magnetic resonance (NMR) spectrometer equipped with a low rf level Robinson oscillator operating in the 10–30 MHz range[1] or EPR spectrometer in GHz range. Magnetic field modulation and lock-in detection customarily used in CW NMR and EPR spectrometers result in the derivative dP/dH of the dissipated rf or microwave power $P(H)$ being recorded as a function of the field at different temperature. In this method it is very difficult to get the exact value of power absorption at a particular temperature, only the relative value of power being absorbed by the sample as a function of magnetic field is possible. Temperature dependent power absorption is also not possible in these methods. We have developed a radio frequency power absorbed measurement technique based on an IC oscillator. In this measurement techniques we can measure absolute power being absorbed by the sample as a function of both magnetic field and temperature.

The combination of high critical temperature, short coherence length and quasi-two-dimensional electronic properties of the copper oxides based superconductors leads to a rich variety of phenomena in the mixed state.[3] Study of the behavior of the mixed state in such systems is of fundamental interest from the view point of understanding the statistics and dynamics of strongly interacting vortices subjected to thermal and structural disorders. Undoubtedly, such studies are also of great technological interest as a variety of electromagnetic applications for high T_c superconductors have been envisaged. Since the microwave and rf power absorption in a superconductor is completely depends on its grain boundary weak links and vortex state it may be very high or very low[4] depending on the state of matter, special techniques are required to study the rf response of superconductors. We have successfully used this technique to measure superconducting transitions in high T_c superconductors and also to study the vortex dynamics of high T_c superconductors under different experimental condition of field, temperature and orientation.

We also found this technique very useful for studying giant magnetoresistance (GMR) and colossal magnetoresistance (CMR) materials. The details of these studies are described in this paper. Here it is demonstrated for the first time

[a)]Author to whom correspondence should be addressed; electronic mail: subhasis@physics.iisc.ernet.in

that one can investigate the magnetic properties of CMR and GMR materials using this technique. The NRRA measurements in this technique were performed at several temperatures between 4 K and 400 K and in the presence of magnetic field up to 1.4 T.

II. OPERATING PRINCIPLE AND CIRCUIT DESIGN

The technique involves placing the sample in the coil which is a part of a *LC* circuit of resonant frequency *f* in the rf range and measuring the change in the total current flows in the circuit. When physical properties of the sample changes the rf energy absorbed by the sample also changes which can be a function of temperature, magnetic field, sample orientation or the resonant frequency itself. According to the rf energy absorbed by the sample the total current supply to the circuit changes. At a particular stage the product between the change in current $\Delta I(I_1 - I_0)$ and the supply voltage V is the net power being absorbed by the sample. Here I_1 is the current supply to the oscillator circuit when sample is present inside the coil L and I_0 is the current when the coil is empty. In our case we keep the voltage V always 5 V for general experiments. We can vary this voltage from 3 V to 20 V depending on the rf power needed for the experiment.

The sensitivity and stability of this technique depend completely on the oscillator. The operating principle of a rf oscillator is very simple. The oscillators work on a form of instability caused by a regenerative feedback without the input dies out due to energy losses. Reactive element in a positive feed back circuit causes the gain magnitude and phase shift to change with frequency. In general, there will be only one frequency corresponding to which the gain magnitude is unity and the phase shift is equivalent to 0°/360°. This satisfies the basic criteria for production of sustained oscillations. An *LC* tank circuit is maintained at a constant amplitude resonance by supplying the circuit with external power to compensate dissipation.

The shift in current is measured with digital multimeter (Keithley 2002 model), which has dc current measurement sensitivity of 10 pA. The fluctuation introduced due to electrical and thermal noise is taken care of by measuring the mean of 50 data points. The above measurement can also be done by any sensitive voltmeter. Here we need to convert the current to voltage by passing the current through a known resistance. The resistance should be lower in value so that it will not restrict the supply current to the oscillator. Typically 1 Ω is a good selection for the resistance value.

Proper grounding is one of the crucial factors influencing the measurement accuracy. The best way is to create only one ground point to which all instruments are connected. The fewer electronics instruments involved in the setup the better, as instrument have their own grounds at different potentials. Connection of instrument creates ground loops and ground loop currents. We recommend using the analog ground of all the instruments ground, not the line ground. As this setup is very sensitive towards ground problem, it is very important to connect all the metallic part of the cryostat and the helium dewar to the same ground.

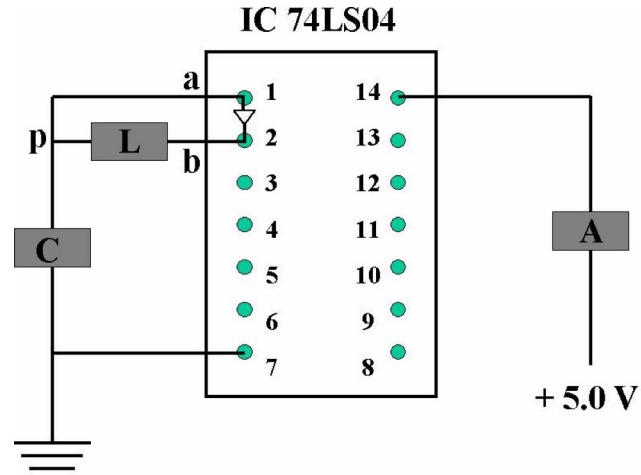

FIG. 1. rf oscillator circuit with IC 74LS04.

Figure 1 shows the oscillator circuit using 74LS04, i.e., TTL bipolar Hex inverter. It is easily available, cost effective and devoid of any biasing problems. The current in the inductor and hence the field H_f can be varied by changing the input voltage at pin 14 of the device. 74LS04 contains six NOT gates with typical propagation delay time ≈15 ns. This specifies the upper limit for its application as a high frequency oscillator. If the voltage at point "a" is low, then output at 2 (point "b") is high and the current builds up in the inductor which in turn transfers its energy to the capacitor. Due to charging of capacitor, voltage at "a" develops to high state and output at "b" becomes low and this leads to sinusoidal oscillations. The frequency of oscillation is given by series *LC* circuit and is given by the standard expression $\omega = 1/(2\pi\sqrt{(LC)})$.

The tank inductance L and capacitance C are vital components of the ICO and have to be chosen with utmost care. For C, surface mount high-Q rf chip capacitor (American Technical Ceramics) with values ranging from 50 to 2000 pF were tried out. Note that it is important to have the value of C higher than the capacitance of the 1.5-ft. RG402 coaxial assembly, which is rated at 29 pF/ft. The inductive coil is a 15-turn solenoid hand-wound using AWG30 insulated Cu wires around a hollow ceramic tube (0.8 cm diameter) and potted with polystyrene epoxy resin. A coating of GE varnish is also applied for good thermal conductivity. Coils with various diameters and wire thickness were tested for stable performance of the tank circuit. Best result were obtained for typical inductance value of $L = 2-9$ μH. The output of this circuit is considerable high, typically 0.7 V with 5 V input and therefore the circuit can be used for gathering information on different type of losses.

III. LOW TEMPERATURE CRYOSTAT

The versatility of the experiment is greatly enhanced when it is adapted to conduct measurements on materials over a wide range in temperature, magnetic field and frequency. This is achieved in our system through integration of our home build circuitry with a customized cryogenic user probe that fits into the commercial Oxford liquid helium cryostat. A semirigid coaxial cable assembly is attached to the

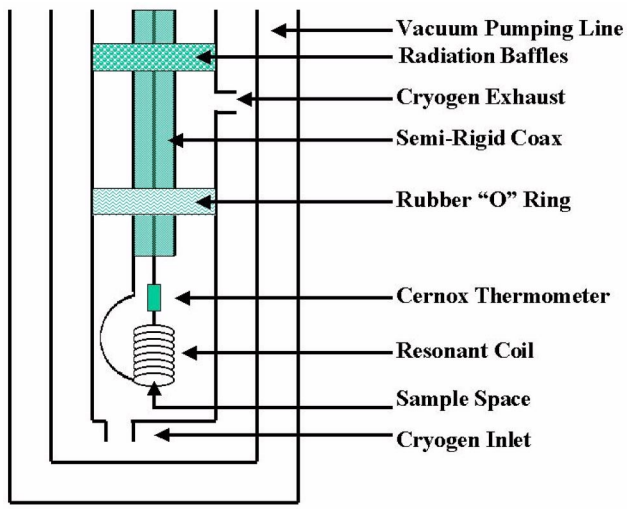

FIG. 2. Schematic of the low temperature probe showing the sample region.

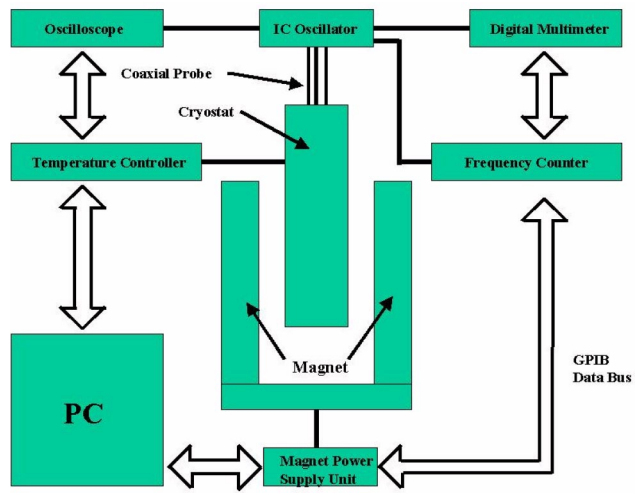

FIG. 3. Layout of the complete ICO measurement system displaying computer control and data acquisition stages.

probe. The inductive coil L from the circuit shown in Fig. 1, is connected to the bottom end of the coaxial cable while the top end is terminated by a female connector that can mated to the rest of the oscillator circuit. A schematic of the coaxial probe that is in the temperature and field controlled region is shown in Fig. 2.

Samples are placed in gelcaps and inserted into the resonant coil. They are securely fastened with Teflon tape to ensure rigidity. The sample and coil are in thermal contact with the temperature sensor (Cernox). Thermal contact is made using Apiezon "N" grease. The coax is fixed in the central bore of the user probe. A double "O" ring seal at the top flange (not shown) is used to maintain a vacuum seal around the coax cable. The inner conductor and the outer shielding are used for electrical connections. Such an arrangement requires only one cable but the coax must be electrically isolated from the surrounding environment. Electrical isolation was obtained by wrapping the coax in Teflon tape and placing a small rubber "O" ring close to the base of the coax. Once the sample and coax were mounted in the user probe, the probe was then inserted into the cryostat. The Oxford temperature controller and the Bruker Electro magnet are then used as a platform for varying the sample temperature ($4\ \mathrm{K} < T < 400$) and static magnetic field ($0 < H < 1.4$).

Thus, our design combines the easy of operation of the temperature controller (including the possibility of changing samples without warming up the system) and its versatile temperature and static magnetic field control, with the oscillator setup.

IV. COMPUTER INTERFACE AND DATA ACQUISITION

Control of the temperature, magnetic field, frequency was through using the standard software and a data acquisition computer. Sequences can be written that would control the temperature and field as a function of time. The analog output ports of the Gauss meter and Cernox censor were utilized as monitors for the field and temperature. The signals were then connected to the 2002-multimeter. Here the 2002-multimeter not only measure the supply current but also measure the dc voltage coming from Gauss meter for magnetic field measurement and resistance of Cernox censor for temperature measurement. We use a scanner card for all the measurements in 2002-multimeter. It should be noted that this was only used to convert analog level to general-purpose interface bus (GPIB) readable data. This data is read via GPIB interface using the same data acquisition computer. The same computer also communicates with the frequency counter, multimeter, oscilloscope, temperature controller and magnet power supply unit.

A typical run would have the scan either magnetic field, temperature or frequency over a certain range. The oscillator data acquisition computer would then monitor the GPIB data bus reading temperature, magnetic field, frequency and the change in current, which measure the power being absorbed. A schematic of this arrangement is shown in Fig. 3.

V. SYSTEM PERFORMANCE

Figure 4 shows the output signal trace from the storage oscilloscope with the IC oscillator at a resonant frequency around 2 MHz. A clean nearly sinusoidal waveform is apparent with a peak to peak amplitude around 700 mV. The amplitude can be adjusted by increasing or decreasing the

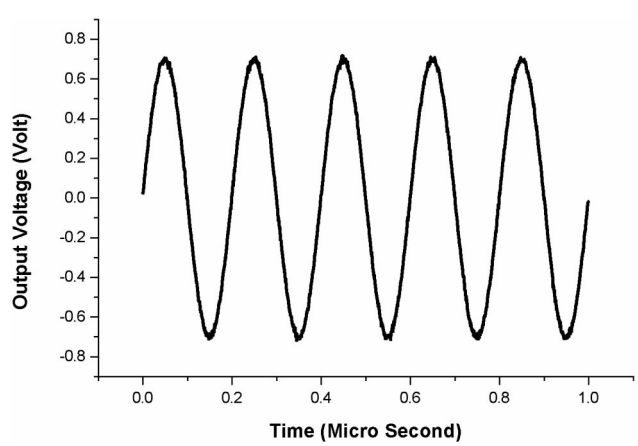

FIG. 4. The output waveform from the ICO circuit measured with a digital oscilloscope. The resonant frequency is around 2 MHz.

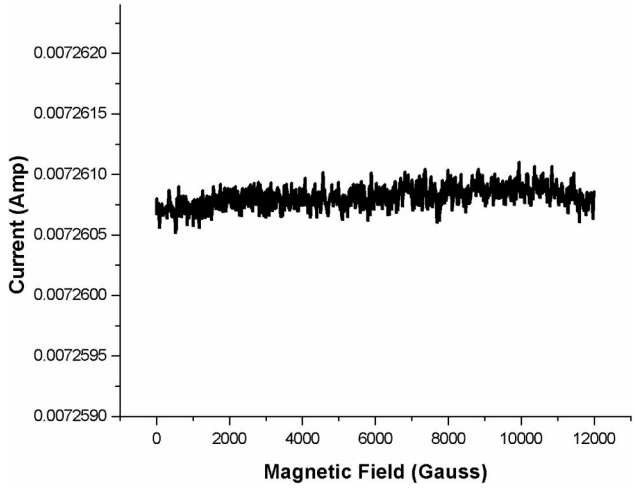

FIG. 5. The current passing in the circuit at 200 K plotted against magnetic field for the empty coil. The duration of field scan is 1 h.

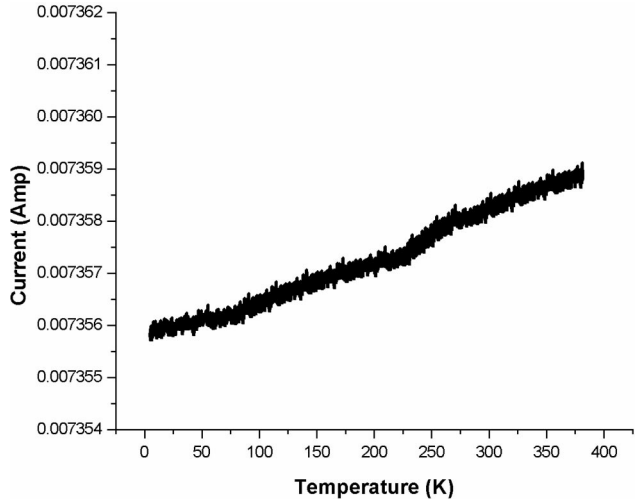

FIG. 7. The current as a function of temperature for the empty coil.

supply voltage. If we change the supply voltage from 5 V to 10 V the rf oscillation amplitude change from 0.7 V to 1.4 V. Changing the inductance L of the coil or the capacitance C of the capacitor changes the resonant frequency.

As mentioned earlier, the experiment depends crucially on the stability of the oscillators. In Fig. 5 we show the stability of the ICO circuit during a typical magnetic field scan. It is taken at 200 K by ramping the field in the steps of 50 mA up to 45 A and back to zero in 1 h. The maximum current (45 A) corresponds to a dc field of 14 kG for 8.4 cm pole separation. Figure 5 also reflects the negligible drift of the oscillation with time. The 4 μA fluctuation is insignificant compared to the magnitude of the effects, that is a current shift of 2.5 mA at the superconducting transition (Fig. 9) and 120 μA at the CMR transition (Fig. 13) in LSMO. Long term stability tests of the ICO were conducted and our circuit showed excellent stability. Drift in the resonant frequency ($\sim$1 KHz) is limited to 1 μA over a period of 20–30 min. Tests over a 24 h period established an overal drift around 5 μA (Fig. 6).

The temperature dependence shown in Fig. 7 is a combined result of decrease in resistivity of the Cu wire making up the coil and the effect of thermal contraction, as the temperature is lowered. In Fig. 8 we show the power drift with frequency. The frequency is varied with only changing C and keeping the amplitude of rf oscillation constant. This shows very minute change in current with frequency. All the above experiments for system performance were done in the absence of any samples.

It is difficult to track down the precise source for all these drifts as several factors can contribute. Some possible candidates include drift in the bias supply, IC operation, and thermal dissipation inside the confined Al box. Nevertheless, these small drifts are at least a few order of magnitudes less than typical current shift encountered in a measurement and do not affect the result. It must be mentioned, however, that an order of magnitude improvement in stability can be achieved by giving proper ground to the metallic part of liquid helium cryostat and the liquid helium dewar.

Both the temperature and field dependence of current shift for the coil are quite repeatable and not very different for the two cases viz., coil axis parallel or perpendicular to

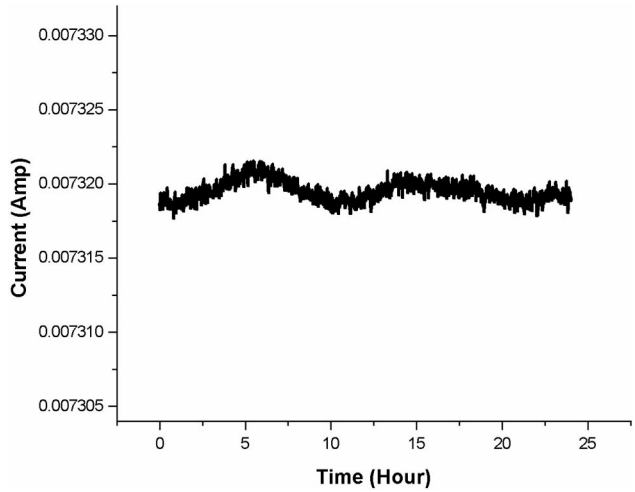

FIG. 6. The current passing in the circuit when coil is empty against time. This is a full day experiment.

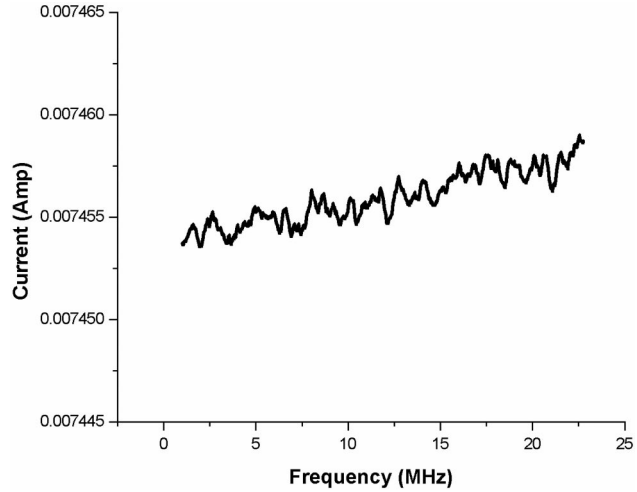

FIG. 8. The current passing in the circuit at room temperature against resonant frequency of the oscillator.

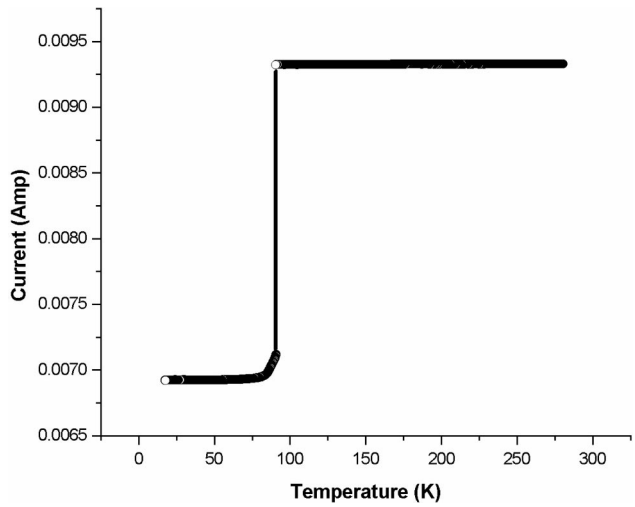

FIG. 9. Measured zero-field temperature dependence of the current for the YBCO (sample 1). The critical temperature T_c is 91 K.

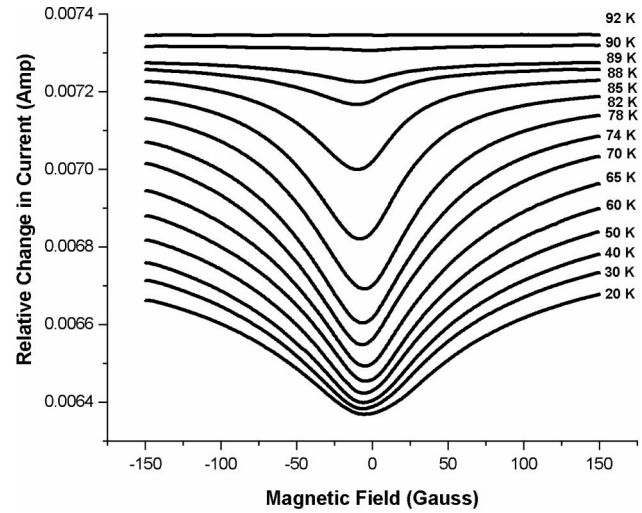

FIG. 10. Field dependence of current for the YBCO (Sample 1) above and below the critical temperature T_c. The magnetic field is scanned from −150 Gauss to +150 Gauss in 60 s.

the dc field provided by the magnet. As a precaution, it should be noted that if the coil is not rigid mounted, one may have to contend with movement of the coil due to Lorentz force acting on it when the oscillating rf field (and hence the rf current) is perpendicular to the applied static field.

VI. DATA AND MEASUREMENTS

In our first experiment we investigated in the high T_c cuprate superconductor YBCO. We prepared two pellets made off polycrystalline samples of YBCO. Both the pellets were exactly similar in size but prepared with different techniques. Both the samples show sharp superconducting transition temperature at ~91 K as determined by $\rho \sim T$ and ac susceptibility measurements. The material was found to be single phasic as determined by x-ray diffraction. The samples were placed in the coil. The filling factor of these samples was ~0.7. At zero fields the noise in measuring supply current was less than 1 μA. The superconducting transitions are clearly visible in both the sample (Fig. 9 and Fig. 11) with the background (discussed above) neglected. One sample (Sample 1) shows the rf power absorption is less in superconducting state than normal state (Fig. 9) whereas the other sample (Sample 2) shows the power absorption is more in the superconducting state than the normal state (Fig. 11). Figure 9 shows that in normal state the supply current value is 9.328 mA and superconducting state the supply current is 6.915 mA. From these values we can easily say that in normal state, the sample (Sample 1) absorbs (~12 mW, multiplication of supply voltage with the change in current) energy more than its superconducting state. Figures 10 and 12 are the magnetic field dependent power absorption at various temperatures in both the samples. Here we have plotted the relative change in current instead of exact value of current just to visualize the change due to field at different temperature. One sample show the rf power absorption increases with increasing field whereas the other one shows power absorption decreases with increasing field. Here it is necessary to note that an increase in current value practically means that the rf oscillations are damping very fast and to sustain the oscillation more current has to be supplied. So more power absorption leads to more supply current to the oscillator. For the Sample 1 the power absorption smoothly and monotonically increases with increasing applied field and shows a tendency to saturate at higher fields. We ascribe this change to be directly associated with the Josephson junction decoupling[5] and flux motion[6] in high T_c superconductors. The shape of the curves and the opposite behavior in these two samples are associated with flux creep, flux flow, Josephson junction critical current, number density of Josephson junctions, and the applied frequency.

Among the two superconducting samples, Sample 1 is the standard superconducting sample, which shows the rf power absorption is less in superconducting state than normal state (Fig. 9). Sample 2 is specially prepared sample to enhance the number density of Josephson junction and the grain boundary weak links. Due to the large number of Josephson junction decoupling in Sample 2 it shows the rf power absorption is more in superconducting state than nor-

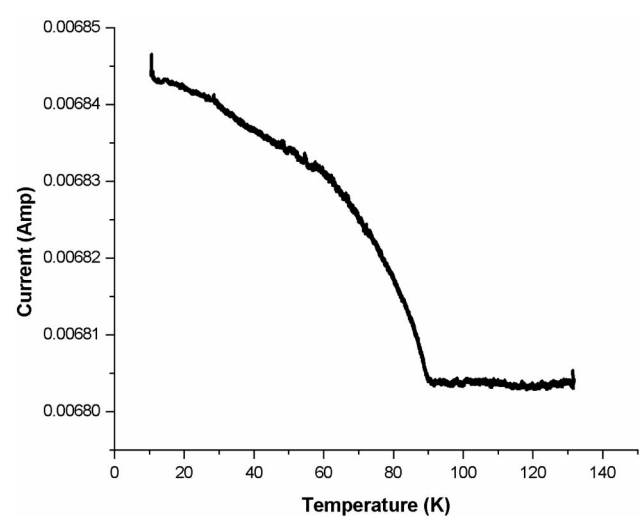

FIG. 11. Measured zero-field temperature dependence of the current for the YBCO (Sample 2). The critical temperature T_c is 91 K.

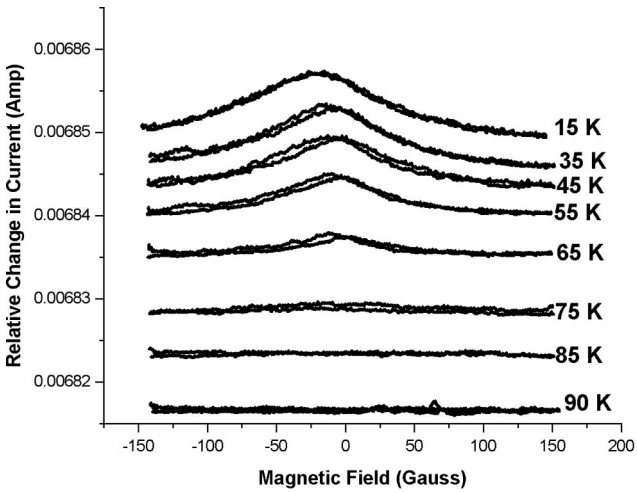

FIG. 12. Field dependence of current for the YBCO (Sample 2) above and below the critical temperature T_c. The magnetic field is scanned from −150 Gauss to +150 Gauss in 60 s.

mal state (Fig. 11). Detail interpretation of the result and a comparison of preparation techniques which leads to different type of power absorption are beyond the scope of this instrumentation article and will be discussed in the forthcoming publication.[7]

In our second experiment we investigated with manganites sample. The ICO based NRRA measurements on manganites sample, $La_{0.7}Sr_{0.3}MnO_3$ (LSMO), are presented in Figs. 13 and 14. This system was recently synthesized and its magnetic and magnetotransport characteristics were studied at our institute. The sample undergoes a paramagnetic to ferromagnetic transition as the temperature is lowered with the Curie temperature T_c around 362 K. In the ICO experiment, the LSMO material is pelletized to capsule form so that it fits snugly into the core of inductive coil. Figure 13 shows the temperature dependence of the power absorbed in zero field. Note that the change in current is much larger than the background shifts due to empty coil and this has been eliminated in the data presented in Figs. 13 and 14. The paramagnetic to ferromagnetic transition is distinctly seen (Fig. 13) and the

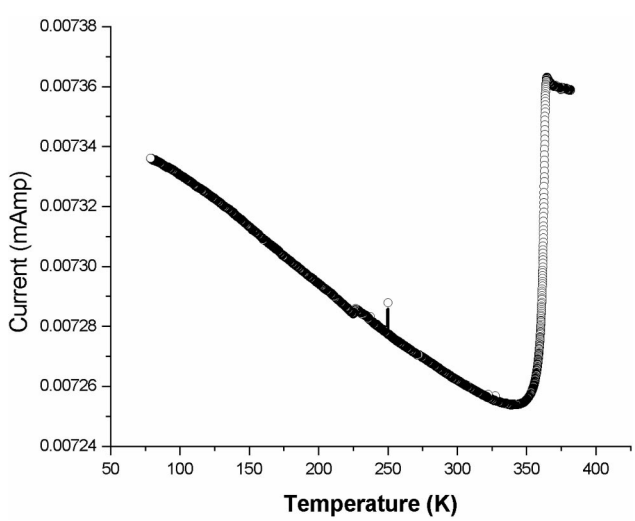

FIG. 13. Measured zero-field temperature dependence of the current for the LSMO sample. The paramagnetic to ferromagnetic transition at 362 K.

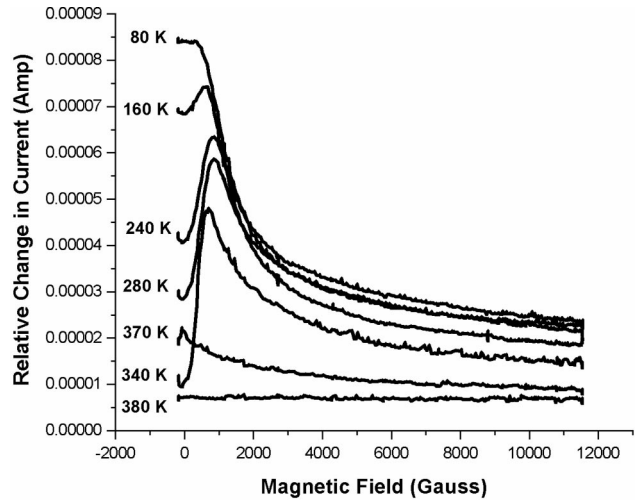

FIG. 14. Field dependence of current for the LSMO sample above and below the ferromagnetic transition temperature T_c. The magnetic field is scanned from −150 Gauss to +150 Gauss in 60 s.

data are consistent with the existing reports on this material.[8,9] In paramagnetic state the sample absorbs more energy than its ferromagnetic state. The field dependence for the same sample is plotted in Fig. 14 where we have shown the data for two cases where the temperature is held above and below T_c. The striking difference in the current variation in the paramagnetic and the ferromagnetic phase of the sample is quite obvious. For $T > T_c$, the current value smoothly and monotonically decreases with increasing applied field and shows a tendency to saturate at higher fields. We ascribe this change to being directly associated with the magneto impedance (MI) which is dominated by rapid change in the permeability. The shape of the curve for $T < T_c$ and the saturation field are different from that seen in the curve for $T > T_c$. For $T < T_c$, the magnetic field dependent power absorption goes through a peak and then saturates. Details interpretation of the results and a comparison of the power absorption for these systems are beyond the scope of this instrumentation article and will be discussed in a forthcoming publication.[10]

VII. DISCUSSION

We have demonstrated a contactless method for measuring conducting, magnetic and trasport properties of materials at different temperature and magnetic field by using this ICO based techniques. Many improvements will enhance this ICO method in future. Use of tunnel diode oscillator in place of IC oscillator may give better stability and resolution. The technique can be useful for the calculation of ac self-field loss in rf reason. Preliminary results on CMR and superconducting samples indicate that this instrument provides a novel way to study the spin and charge dynamics in CMR materials and Josephson junctions and vortex phenomena in superconducting materials.

ACKNOWLEDGMENTS

S.V.B. would like to thank CSIR, UGC, and DST, India for financial support.

[1] S. V. Bhat, P. Ganguly, T. V. Ramakrishnan, and C. N. R. Rao, J. Phys. C **20**, L559 (1987).
[2] A. Rastogi, Y. S. Sudershan, S. V. Bhat, A. K. Grover, Y. Yamaguchi, K. Oka, and Y. Nishihara, Phys. Rev. B **53**, 9366 (1996).
[3] G. Blatter, M. V. Feigel'man, V. B. Geshkenbein, A. I. Larkin, and V. M. Vinokur, Rev. Mod. Phys. **66**, 1125 (1994).
[4] W. H. Hartwig and C. Passow, *Applied Superconductivity*, edited by V. L. Newhouse (Academic, New York, 1975), Vol. II.
[5] A. Dulcic, B. Rakvin, and M. Pozek, Europhys. Lett. **10**, 593 (1989).
[6] A. M. Portis, K. W. Blazey, K. A. Muller, and J. G. Bednorz, Europhys. Lett. **5**, 467 (1988).
[7] S. Sarangi, S. P. Chockalingam, and S. V. Bhat (unpublished, 2004).
[8] S. Y. Yang, W. L. Kuang, Y. Liou, W. S. Tse, S. F. Lee, and Y. D. Yao, J. Magn. Magn. Mater. **268**, 326 (2004).
[9] A. K. Debnath and J. G. Lin, Phys. Rev. B **67**, 064412 (2003).
[10] S. Sarangi, S. S. Rao, and S. V. Bhat (unpublished, 2004).